Progress In Electromagnetics Research, Vol. 110, 297–311, 2010

AN ARBITRARY CONFORMAL ARRAY PATTERN SYNTHESIS METHOD THAT INCLUDES MUTUAL COUPLING AND PLATFORM EFFECTS

Q. Wang

Communication Engineering Department
Nanjing Institute of Technology, Nanjing 211167, China

Q.-Q. He

Southwest China Institute of Electronic Technology
Chengdu 610036, China

Abstract—The research in the paper puts forward a novel method for synthesizing conformal arrays and optimizing low cross-polarizations including the effects of elements mutual coupling and mounted platform. Starting from the far-field superposition principle, an efficient approach with active element pattern technique is proposed to calculate the far-field patterns. A coordinate transform is used to create polarization quantities, and a general process for the element polarized pattern transformation is proposed. The two numerical examples are proposed, and the desired sidelobe levels and low cross-polarizations are optimized. Numerical results indicate the proposed method is valid.

1. INTRODUCTION

Conformal arrays have good potential for application in aerospace vehicles with excellent aerodynamic characteristics. Because conformal arrays generally are curved, new far-field behaviors emerge [1–5], and most of the traditional linear and planar array synthesis methods are not valid. A variety of techniques have been used to solve the synthesis problem for conformal array, such as interpolation technique [6], space mapping technique [7], non-linear optimization method [8], intersection approach [9], least squares methods [10], simulated annealing technique [11], adaptive array theory [12], and

Received 22 September 2010, Accepted 15 November 2010, Scheduled 23 November 2010
Corresponding author: Qi Wang (yc_wq@163.com).

particle swarm optimization [13]. Furthermore, in the design of conformal arrays, problems arise, which are different from those appearing in arrays on planar surfaces. The polarization in the far field changes as a function of directional angle for radiating elements whose polarization is fixed with respect to the surface of the platform [14]. In [15], adaptive array theory is applied to a conformal antenna array to synthesize a main beam with optimized polarization employing dual polarized patch antennas as radiators. Wang et al. [16] have investigated low cross-polarization optimization by using the alternating projection method. However, these synthesis techniques mentioned above mostly neglect the element mutual couplings, and the effect of mounted platform is also not rigorously taken into account.

In the paper, this research presents a new method to synthesize arbitrary conformal arrays including the effects of mutual coupling and mounted platform. With active element pattern technique [17], a conformal array model is firstly created and polarization quantities with Euler rotation [18] for each element are obtained. Different from the axis rotations in [16], plane rotations are proposed to realize the element polarization transformation. In order to obtain the good cross-polarization and side lobe levels, a genetic algorithm (GA) [19, 20] is used, and different from [21, 22], the curved-face conformal arrays are investigated and GA combining with an active element pattern technique is used to calculate the complicated radiation pattern function. Numerical results show the proposed method is feasible and valid.

2. THEORIES

As a rule, the total radiated field of an arbitrary array can be expressed by applying the principle of superposition

$$\mathbf{E}(\theta,\varphi) = \sum_m \sum_n w_{mn}\mathbf{F}_{mn}(\theta,\varphi)e^{jk\hat{\mathbf{r}}\cdot\mathbf{R}_{mn}} \tag{1}$$

where $m = 1, 2, \ldots, M$; $n = 1, 2, \ldots, N$; w_{mn} is the excited complex current applied to the mnth element; M is the number of stacked arc subarrays and N is the number of radiators in the mth arc subarray; $\mathbf{F}_{mn}(\theta,\varphi)$ is the active element pattern of the mnth element, $e^{jk\hat{\mathbf{r}}\cdot\mathbf{R}_{mn}}$ is the spatial phase term, $\hat{\mathbf{r}}$ is the unit radial vector from the coordinate origin to the observation direction (θ,φ), and $\mathbf{R}_{mn}$ is a position vector from the origin to the center of the mnth element; boldface type indicates a vector quantity. Usually, $\mathbf{F}_{mn}(\theta,\varphi)$ in (1) is different from the isolated element pattern because other elements will radiate some power due to the effects of element mutual coupling

and mounted platform. Furthermore, $\mathbf{F}_{mn}(\theta, \varphi)$ also depends on the polarization of the array element and the position of the array element. In the active element pattern approach, the effects of mutual coupling and mounted platform are accounted for through the active element. The active element pattern $\mathbf{F}_{mn}(\theta, \varphi)$ is obtained by exciting only the mnth element and loading all other elements with the matched impedances. The active element pattern arises from direct radiation from the mnth element combined with fields reradiated from the other elements associated with the surrounding array environment. Thus the total radiated field of an arbitrary array that includes the effects of mutual coupling and mounted platform can be computed based on the active element pattern approach.

Generally, the whole array radiating field in (1) can be divided into a co-polarization quantity and cross-polarization quantity. Thus the total field may be rewritten as follows

$$\mathbf{E}(\theta, \varphi) = \mathbf{E}_{co}(\theta, \varphi) + \mathbf{E}_{xp}(\theta, \varphi) \tag{2}$$

where $\mathbf{E}_{co}(\theta, \varphi)$ is the co-polarization quantity and $\mathbf{E}_{xp}(\theta, \varphi)$ is the cross-polarization quantity.

Obviously, the unusual geometry of the conformal array requires special consideration of the coordinate system used to represent the patterns. In order to easily obtain the far field pattern of the conformal array, the coordinate transformation for element pattern between the element local coordinate system and the global coordinate system needs to be carried out to count the contribution of each element to the

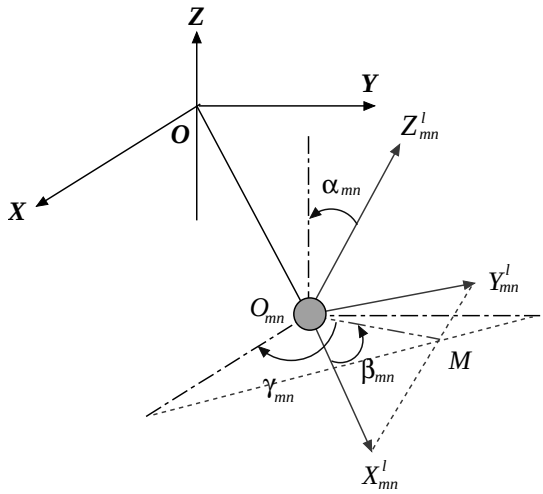

Figure 1. Corresponding coordinate system for element radiators.

conformal array radiation. The corresponding transformation relation from the local coordinate system to the global coordinate system is shown in Figure 1.

In Figure 1, the local coordinate system is defined by $O_{mn} - X^l_{mn}Y^l_{mn}Z^l_{mn}$, and the superscript "$l$" represents the local coordinate system. Z^l_{mn}-axis of local system is oriented along the direction of the local normal vector of curved surface where the mnth element is placed. The directions of X^l_{mn}- and Y^l_{mn}-axis are determined by the particular position of the mnth element. Thus the transformation from the local coordinate system to the global coordinate system can be obtained as follows

$$\begin{bmatrix} X \\ Y \\ Z \end{bmatrix} = \begin{bmatrix} X_{O_{mn}} \\ Y_{O_{mn}} \\ Z_{O_{mn}} \end{bmatrix} + \mathbf{R}(\beta_{mn}, \alpha_{mn}, \gamma_{mn}) \begin{bmatrix} X^l_{mn} \\ Y^l_{mn} \\ Z^l_{mn} \end{bmatrix} \tag{3}$$

where $(X_{O_{mn}}, Y_{O_{mn}}, Z_{O_{mn}})$ is the mnth element position in the global coordinate system, $\mathbf{R}(\beta_{mn}, \alpha_{mn}, \gamma_{mn})$ is a 3×3 Euler rotation matrix [18].

For certain applications, the conformal array patterns are usually designed to have low sidelobe and low cross polarization. But conformal array factor often can not be separated because of the effects of structure curvature, and the traditional linear/planar array synthesis methods often do not apply to curved arrays. Thus the pattern synthesis and low cross polarization optimization for conformal array need powerful and attractive methods. Furthermore, the placement of an element will be greatly influenced by the shape of the mounted platform. Instead, if individual element patterns, which include the effects of the mounted platform and mutual coupling, are used, a more general superposition computation must be performed in the whole area. Simultaneously, the co-polar and cross-polar patterns in the far field change as a function of directional angle for radiating elements whose polarization is fixed with respect to the surface of the platform. With the curvature effect, the cross-polar quantities will be possible to exceed the co-polar quantities in certain locations, and increase largely the array losses, thus the polarization optimization needs to be implemented. One possible approach for solving this generalized problem is through the use of GA combining with active element technique to select the excitation magnitudes and phases that can produce the closest possible match to a desired array radiating patterns. Thus for an arbitrary sidelobe area $S_1(\theta_1, \varphi_1)$ and mainbeam area $S_0(\theta_0, \varphi_0)$ in (2), the optimized target of the co-polarization pattern is reducing the sidelobe level, and the target of the cross-polarization pattern is the maximum of cross-polarization level is desired to reach the ideal case comparing with the maximum of co-

polarization pattern. Thus, the fitness function of conformal array can be given by

$$f(w_{mn}) = \mu_1 \left| \max_{(\theta,\varphi)\in S_1(\theta_1,\varphi_1)} [SLL_{co}(\theta,\varphi)] - SLVL_1 \right| + \mu_2 \left| \left\{ b - \max_{(\theta,\varphi)\in S_0(\theta_0,\varphi_0)+S_1(\theta_1,\varphi_1)} [SLL_{xp}(\theta,\varphi)] \right\} - SLVL_2 \right| \quad (4)$$

where $w_{mn} = (w_{co,\,mn}, w_{xp,\,mn})$ is the excited weight and can be found in (1). $w_{co,\,mn}$ is the co-polarization excited weight of the first part in (4), and $w_{xp,\,mn}$ is the cross-polarization excited weight of the second part in (4). μ_1 is the tuning weight of co-polarization pattern, μ_2 is the tuning weight of cross-polarization pattern. $SLVL_1$ is a desired co-polarization sidelobe level, $SLVL_2$ is a desired cross-polarization level, SLL_{co} is the co-polarization sidelobe level, SLL_{xp} is the cross-polarization level, and b is the maximum of the co-polarization pattern and given by

$$b = \max_{(\theta,\varphi)\in S_0(\theta_0,\varphi_0)} [|\mathbf{E}_{co}(\theta,\varphi)|] \quad (5)$$

In (4), the first part expression indicates to let co-polarization sidelobe levels reach the desired low sidelobe level and the second part expression indicates to let cross-polarization levels reach the desired low cross-polarization in the whole space domain. $\max_{(\theta,\varphi)\in S_0(\theta_0,\varphi_0)+S_1(\theta_1,\varphi_1)} [SLL_{xp}(\theta,\varphi)]$ is the max level of the cross-polarization pattern, and $\{b - \max_{(\theta,\varphi)\in S_0(\theta_0,\varphi_0)+S_1(\theta_1,\varphi_1)} [SLL_{xp}(\theta,\varphi)]\}$ is the normalization level of the cross-polarization pattern referring to the b. In implementing the GA algorithm process, each individual of each generation can be expressed as a group of the excited weight. For the co-polarization pattern, b can be calculated based on the $w_{co,\,mn}$, and then b is seen as the benchmark for optimizing the cross-polarization pattern in the second part of (4). If the first part of (4) cannot reach the optimized target in the tuning process, μ_1 is increased, and vice versa, μ_2 is increased. Here, the tuning factors μ_1 and μ_2 are [0.5 1.5] and [0.4 1], respectively.

3. EXAMPLES AND NUMERICAL RESULTS

3.1. Three-dimension Transformation of Conformal Array

Generally, the three-dimension polarized transformations of conformal arrays include conical array, spherical array, paraboloidal array, and other complicated shaped surface array. Here, a conical array is

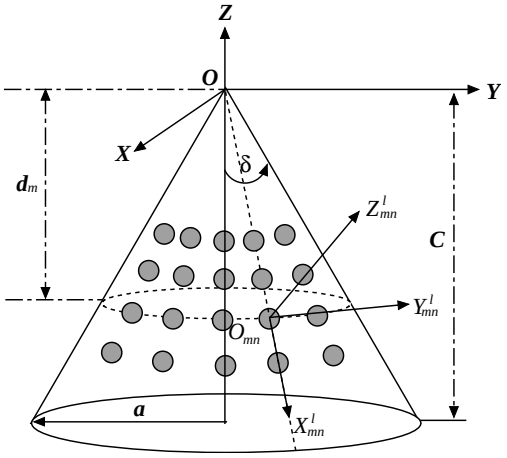

Figure 2. Geometry of conformal conical array.

implemented to validate the proposed method. For the conical surface as shown in Figure 2, its curved surface equation is

$$z = -\frac{c}{a}\sqrt{x^2 + y^2} \tag{6}$$

where constant c is the cone high and constant a is the bottom radius, cone angle δ is determined by $\arctan(a/c)$. Thus, for the mth arc subarray, the arc radius is

$$r_m = d_m \tan\delta \tag{7}$$

where d_m is the distance from origin of the global coordinate system to the mth arc subarray plane.

Assumed the spacing between each element is $0.5\lambda_0$ along the radial direction of the conical surface, where λ_0 is the free space wavelength corresponding to an operating frequency of 32 GHz. The bottom radius of the cone is $R = 8\lambda_0$ and the half conical angle is $\delta = 30^\circ$, thus the coordinate of the mth stacked arc subarray is

$$d_m = \left[-\left|\frac{R}{\sin\delta}\right| + (m-1)\frac{\lambda_0}{2}\right]\cos\delta \tag{8}$$

Based on the created rotation relation in (3), α_{mn}, β_{mn}, and γ_{mn}

can be given by mathematical manipulation as follows

$$\alpha_{mn} = \pi/2 - \delta \tag{9}$$

$$\beta_{mn} = \text{ar}\cos\left(\frac{-r_m\cos\varphi_n\cos\varphi_n - r_m\sin\varphi_n\left(\sin\varphi_n - \frac{1}{\sin\varphi_n}\right)}{R^p_{mn}\sqrt{(\cos\varphi_n)^2 + \left(\sin\varphi_n - \frac{1}{\sin\varphi_n}\right)^2}}\right) \tag{10}$$

$$\gamma_{mn} = \arctan\left(\frac{\sin\varphi_n\cos\varphi_n}{\sin\varphi_n\sin\varphi_n - 1}\right) \tag{11}$$

In (10), R^p_{mn} is the distance from the origin of the global coordinate system to the mnth element on the radial direction of the conical surface, and

$$R^p_{mn} = \sqrt{(r_m\cos\varphi_n)^2 + (r_m\sin\varphi_n)^2 + (d_m)^2} \tag{12}$$

Applying (9), (10), (11), and (12), the element pattern polarization transformation can be finished, and the total radiated field can be computed in (2).

Of course, based on the prevalent simulated means of conformal array [23–25], a multifaceted surface can be a very good approximation to the curved counterpart. Here, the conical array is created by using 36 segments multifaceted surfaces. On the each multifaceted surface, the patch radiating element can be designed exactly, as shown in Figure 3.

For each element of the mth stacked subarray in the φ-direction, radiating elements are arranged with an equal angle-spacing, and here the angle-spacing is $\Delta\varphi = 0.075\,\text{rad}$. A microstrip patch with a length of $L = 1.8\,\text{mm}$ and a width of $W = 1.1\,\text{mm}$ is selected as

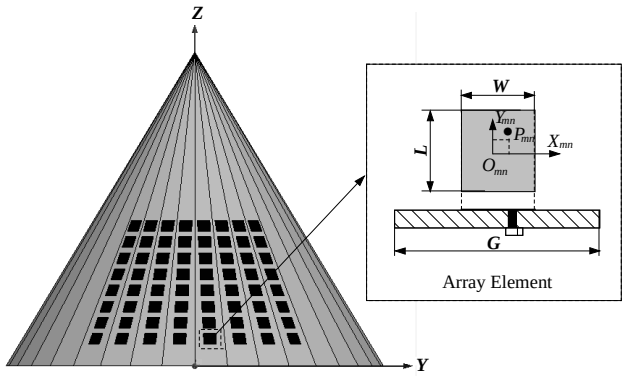

Figure 3. Model of the conformal array and its radiating element.

the radiating element. The ground plane dimensions of the patch antennas are chosen to be $G \times G = 4 \times 4\,\mathrm{mm}^2$. Taconic RF-60 with a thickness $h = 0.508\,\mathrm{mm}$ and a relative permittivity $\varepsilon_r = 6.15$ is used as the substrate. A $50\,\Omega$ probe feed, which is located at the point $P_{mn}(0.25\,\mathrm{mm}, 0.25\,\mathrm{mm})$ separated from the mnth patch center, is used to excite the patch.

Here, an active element pattern technique [17] is used to obtain array element pattern data. The active element pattern technique, which uses the simulated or measured patterns of individual elements in the array environment to calculate the pattern of the fully excited array, can often be employed when classical analysis and numerical techniques cannot. For a conformal array computation, one of the main reasons for the difficulty involved in developing synthesis techniques for conformal array elements mounted on arbitrarily shaped platforms involves the computational burden associated with simulating these antennas in a practical environment (i.e., taking into account the antenna/platform interactions) [21]. Thus, if carrying out the entire array simulation for most cases, it is difficult due to computer hardware limit. An active element pattern technique possesses a good advantage to compute a large array, and it can divide a large array analysis problem as a superposition of various simplified small array problems and greatly reduces the computation burden [26]. Active element patterns are either measured on a test range or are simulated in some manner. With the active element pattern method, the array elements can be divided into edge elements and interior elements. The edge elements are typically taken to be the first and final rows and columns

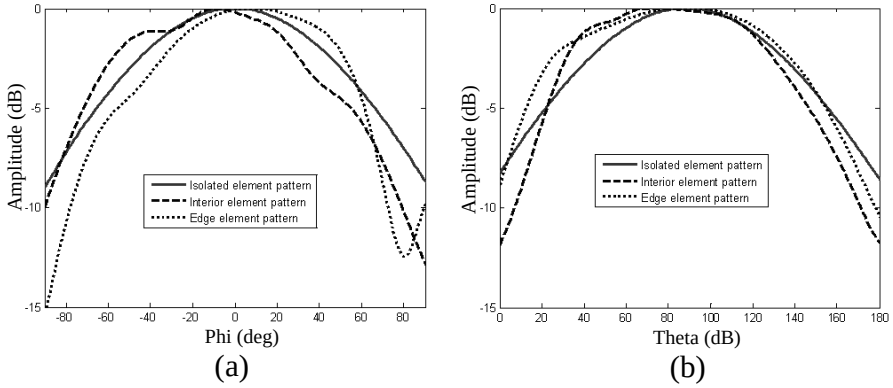

Figure 4. Isolated element pattern and active element patterns. (a) *xoy*-plane; (b) *xoz*-plane.

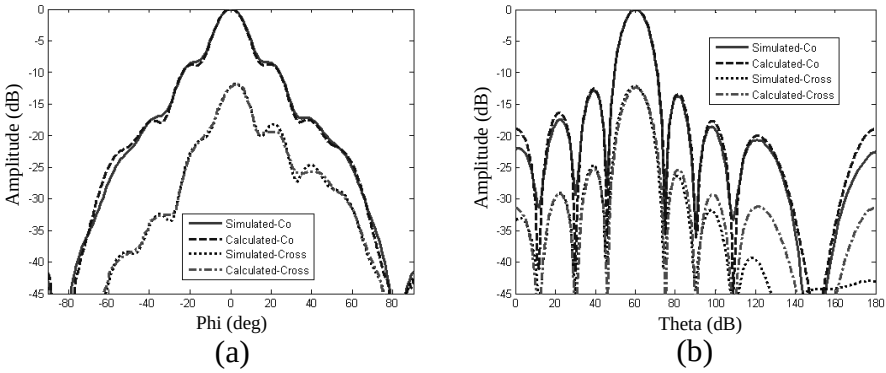

Figure 5. Far-field patterns for the 8×8 conical array based on the proposed method and HFSS simulation. (a) $xoy60$-plane; (b) xoz-plane.

of the active elements on the sides of the conical array. Here, based on the geometrical symmetry about xoz-plane in Figure 3, a half of all elements are simulated. Corresponding active element pattern data about these elements are obtained with a finite element method software HFSS. Figure 4 shows the co-polarization patterns for the isolated element and the active elements. It is clear that these patterns are different because of the effects of element mutual coupling and mounted platform. Similarly, the cross-polarization patterns for the isolated element and the active elements possess same case.

Figure 5 plots the far field patterns for a 8×8 conical array by using the proposed method and HFSS simulation, respectively. Of course, the proposed method not only suits the uniform excited array, but also suits the no-uniform excited array. Here $xoy60$-plane denotes a surface where θ is 60° and φ vary from -90° to $+90^\circ$, and xoz-plane denotes a plane where φ is 0° and θ vary from 0° to 180°. Obviously, it is seen that the results of using the proposed method are consistent with those of HFSS simulation for co-polarization patterns. In the xoz-plane, because of modeling approximations between multifaceted surface and true curve-surface, cross-polarization patterns have different in the range from 110° to 180°. Furthermore, Figure 5 reveals that the curvature plays a significant role for the sidelobe and cross-polarization levels of the conical array patterns. The first sidelobe starts to merge with the main beam and a high cross-polarization level is produced. Thus, in order to compensate for these effects, a GA approach to radiation pattern synthesis is developed. This synthesis technique yields the optimal set of excited current amplitudes and phases required to compensate as much as possible for these effects on the array [2].

In order to obtain good sidelobe and low cross-polarization, the excited weights w_{mn} of (4) need be optimized. For resolving the optimized problem of a large amount of parameters, many optimizing methods can be selected, and here a GA complying with the adaptive rule [19] is selected to implement this optimization. Based on the geometrical symmetry about xoz-plane, the optimized parameters can be reduced half on the whole space domain. The number of the excited amplitudes and phases for the co-polarization quantity are 64 and the number of the excited amplitudes and phases for the cross-polarization quantity are also 64. All excited amplitudes are varied from 0 to 1, and all excited phases are varied from 0 to 2π. The GA is encoded using a population size of approximately 180 members, the crossover and mutation means use the unrepeatable strategies, respectively. After performing the crossover and mutation manipulations, the elites are maintained in order to prevent the losses of the optimized results and accelerate the convergence of this algorithm. For evolutional each generation, the crossover and mutation probabilities comply with the adaptive rule. The target function is defined by the sidelobe level (-20 dB) and cross-polarization level (-30 dB). After about 210 iterations, the resulting patterns with the proposed method are shown in Figures 6 and 7. They are shown that the co-polarization and cross-polarization radiating patterns obtain about -20 dB sidelobe level and -30 dB low cross-polarization level, respectively. Of course, it is obvious that the array gain and the array efficiency descend when the optimization is carried out.

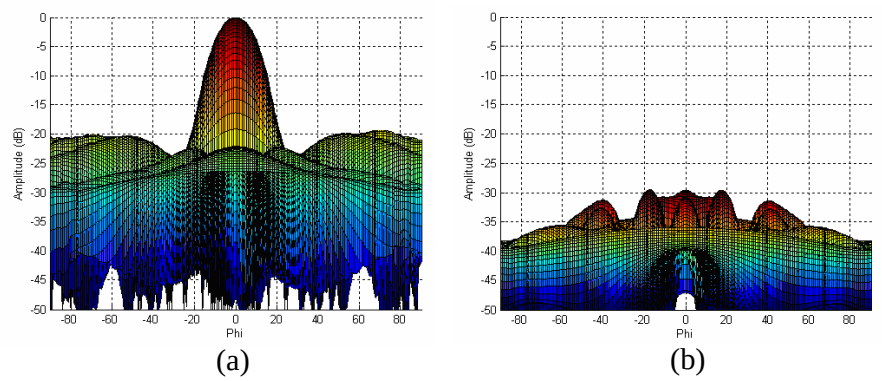

Figure 6. View of the radiating patterns for conical array in the xoy-plane. (a) Co-polarization radiated pattern; (b) cross-polarization radiated pattern.

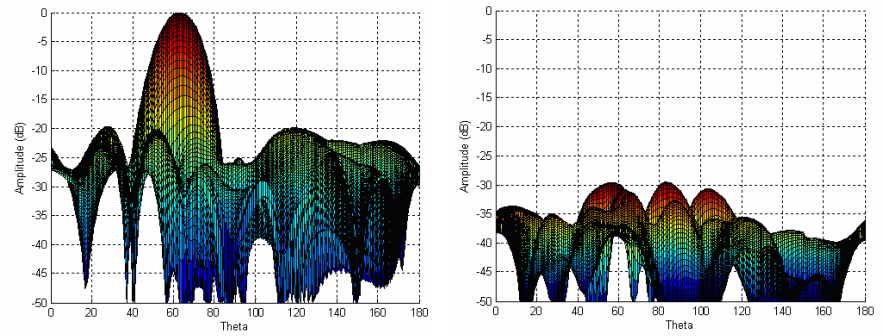

Figure 7. View of the radiating patterns for conical array in the xoz-plane. (a) Co-polarization radiated pattern; (b) cross-polarization radiated pattern.

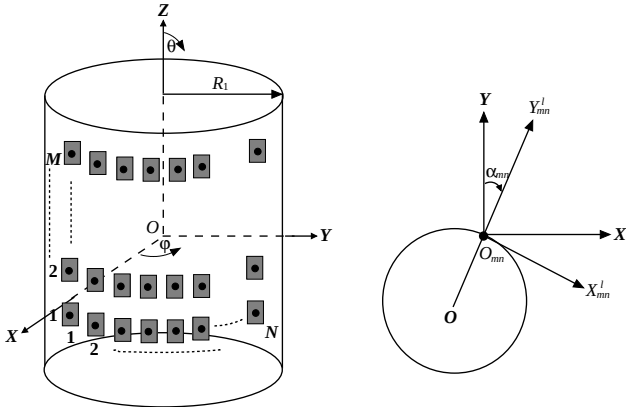

Figure 8. Geometry of cylindrical array and corresponding coordinate system for element radiators.

3.2. Two-dimension Transformation of Conformal Array

Generally, the two-dimension polarized transformations of conformal arrays include cylindrical array, ellipsoidal array, circular array, and arc-line array, etc. In order to further illuminate the ability of the proposed method for computing conformal arrays, a cylindrical array is given as the second example. Here, the spacings between each element is $\Delta\varphi = 0.0698$ rad along the arc-direction of the cylinder and $\Delta d = 0.5\lambda$ along the z-direction of the cylinder, respectively. The topology of cylindrical array is 8×8 as shown in Figure 8, and microstrip

patch is chosen as radiating element which is already given above. The active element pattern data are obtained based on the same method mentioned above. Corresponding element polarized transformation takes place at φ-direction, thus the Equation (3) becomes

$$\begin{bmatrix} X \\ Y \end{bmatrix} = \begin{bmatrix} \sin\alpha_{mn} & -\cos\alpha_{mn} \\ \cos\alpha_{mn} & \sin\alpha_{mn} \end{bmatrix} \begin{bmatrix} X^l_{mn} \\ Y^l_{mn} \end{bmatrix} \tag{13}$$

where $\alpha_{mn} = (n - \frac{N+1}{2})\Delta\varphi$; $n = 1, 2, \ldots, N$; $m = 1, 2, \ldots, M$. Further solving the Equation (13), and have

$$\varphi_{mn} = \varphi^l_{mn} + \alpha_{mn} \tag{14}$$

where φ_{mn} is the polarized-direction at the global coordinate system and φ^l_{mn} is the polarized-direction at the local coordinate system. Based on Equation (14), the element pattern polarization transformation can be performed, and the total radiated fields can be computed in Equation (2).

Similarly, the target function of GA is defined by the sidelobe level (-20 dB) and cross-polarization level (-30 dB). After about 190 iterations, the resulting patterns with the proposed method are shown in Figures 9 and 10. They are shown that the co-polarization and cross-polarization radiating patterns obtain about -20 dB sidelobe level and -30 dB low cross-polarization level, respectively.

Through further calculation and analysis to the two examples, it is found that it is very difficult to define the radiating characteristic plane for conformal array. Thus the pattern optimization for conformal array often need to be performed in the whole space domain.

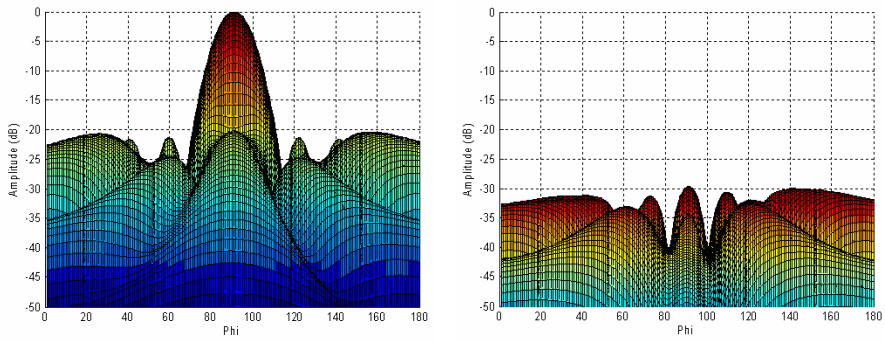

Figure 9. View of the radiating patterns for cylindrical array in the *xoy*-plane. (a) Co-polarization radiated pattern; (b) cross-polarization radiated pattern.

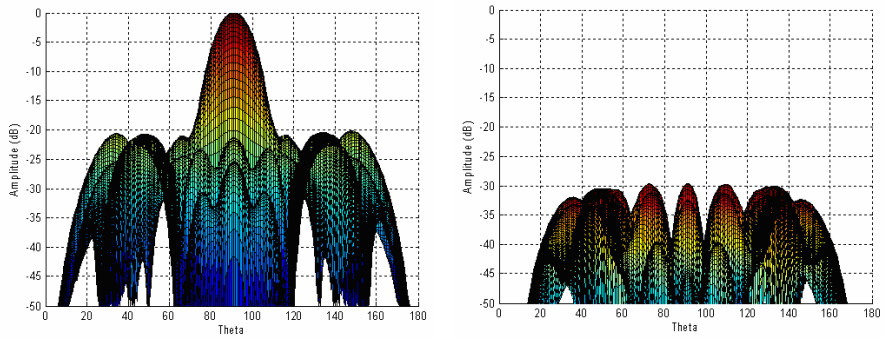

(a) (b)

Figure 10. View of the radiating patterns for cylindrical array in the xoz-plane. (a) Co-polarization radiated pattern; (b) cross-polarization radiated pattern.

4. CONCLUSIONS

In the paper, the research puts forward a novel method for synthesizing conformal arrays and optimizing low cross-polarizations based on the effects of elements mutual coupling and mounted platform. The proposed method can be used for arbitrary conformal arrays including non-uniformly spacing array. The proposed method can also be used for different carriers such as conducting platforms, dielectric platforms, and even material platforms with a relative permittivity of 1. Thus the proposed method has a good engineering application. Numerical results in the paper are provided to demonstrate the effectiveness and behaviors of the proposed method.

ACKNOWLEDGMENT

This work was supported by the Scientific Research Fund of Nanjing Institute of Technology. No. CKJ2009005 and No. KXJ08139.

REFERENCES

1. Zhang, Y. J., S. X. Gong, and Y. X. Xu, "Radiation pattern synthesis for arrays of conformal antennas mounted on an irregular curved surface using modified genetic algorithms," *Journal of Electromagnetic Waves and Applications*, Vol. 23, No. 10, 1255–1264, 2009.

2. He, Q.-Q., H.-D. He, and H. Lan, "An efficient pattern synthesis method for cylindrical phased array antennas," *Journal of Electromagnetic Waves and Applications*, Vol. 23, No. 4, 473–482, 2009.
3. Sun, J. S., D. S. Goshi, and T. Itoh, "Optimization and modeling of sparse conformal retrodirective array," *IEEE Trans. Antenna Propagat.*, Vol. 58, No. 3, 977–981, Mar. 2010.
4. Li, W. T., X. W. Shi, Y. Q. Hei, S. F. Liu, and J. Zhu, "A hybrid optimization algorithm and its application for conformal array pattern synthesis," *IEEE Trans. Antenna Propagat.*, Vol. 58, No. 10, 3401–3406, Oct. 2010.
5. Lu, Z.-B., A. Zhang, and X.-Y. Hou, "Pattern synthesis of cylindrical conformal array by the modified particle swarm optimization algorithm," *Progress In Electromagnetics Research*, Vol. 79, 415–426, 2008.
6. Yang, P., F. Yang, Z.-P. Nie, B. Li, and X. Tang, "Robust adaptive beamformer using interpolation technique for conformal antenna array," *Progress In Electromagnetics Research B*, Vol. 23, 215–228, 2010.
7. Ouyang, J., F. Yang, H. Zhou, Z. Nie, and Z. Zhao, "Conformal antenna optimization with space mapping," *Journal of Electromagnetic Waves and Applications*, Vol. 24, Nos. 2–3, 251–260, 2010.
8. Banach, M. and J. Cunningham, "Synthesis of arbitrary and conformal arrays using non-linear optimization techniques," *Proc. IEEE Radar Conf.*, 38–43, 1988.
9. Mazzarella, G. and G. Panarieello, "Pattern synthesis of conformal arrays," *IEEE AP-S Int. Symp.*, 1054–1057, Jul. 1993.
10. Vaskelainen, L. I., "Iterative least-squares synthesis methods for conformal array antennas with optimized polarization and frequency properties," *IEEE Trans. Antenna Propagat.*, Vol. 45, No. 7, 1179–1185, Jul. 1997.
11. Ferrira, J. A. and F. Ares, "Pattern synthesis of conformal arrays by the simulated annealing technique," *Electron. Lett.*, Vol. 33, No. 14, 1187–1189, Jul. 1997.
12. Zhou, P. Y. and M. A. Ingram, "Pattern synthesis for arbitrary arrays using an adaptive array method," *IEEE Trans. Antenna Propagat.*, Vol. 47, No. 5, 862–869, May 1999.
13. Liu, X. F., Y. C. Jiao, and F. S. Zhang, "Conformal array antenna design using modified particle swarm optimization," *Journal of Electromagnetic Waves and Applications*, Vol. 22, Nos. 2–3, 207–

218, 2008.

14. Hansen, R. C., *Phased Array Antennas*, John Wiley & Sons, Inc., 1998.
15. Dohmen, C., J. W. Odendaal, and J. Joubert, "Synthesis of conformal arrays with optimized polarization," *IEEE Trans. Antenna Propagat.*, Vol. 55, No. 10, 2922–2925, Oct. 2007.
16. Wang, B.-H., Y. Guo, Y.-L. Wang, and Y.-Z. Lin, "Frequency-invariant pattern synthesis of conformal array antenna with low cross-polarisation," *IET Microw. Antennas Propag.*, Vol. 2, No. 5, 442–450, Aug. 2008.
17. Pozar, D. M., "The active element pattern," *IEEE Trans. Antenna Propagat.*, Vol. 42, No. 8, 1176–1178, Aug. 1994.
18. Milligan, T., "More applications of Euler rotation angles," *IEEE Antenna Propagat. Mag.*, Vol. 41, No. 4, 78–83, Aug. 1999.
19. Srinivas, M. and L. M. Patnaik, "Adaptive probabilities of crossover and mutations in genetic algorithms," *IEEE Trans. Antenna Propagat.*, Vol. 24, No. 4, 656–667, Apr. 1994.
20. Xu, Z., H. Li, Q.-Z. Liu, and J.-Y. Li, "Pattern synthesis of conformal antenna array by the hybrid genetic algorithm," *Progress In Electromagnetics Research*, Vol. 79, 75–90, 2008.
21. Allard, R. J., D. H. Werner, and P. L. Werner, "Radiation pattern synthesis for arrays of conformal antennas mounted on arbitrarily-shaped three-dimensional platforms using genetic algorithms," *IEEE Trans. Antenna Propagat.*, Vol. 51, No. 5, 1054–1062, May 2003.
22. Guo, J-.L. and J-.Y. Li, "Pattern synthesis of conformal array antenna in the presence of platform using differential evolution algorithm," *IEEE Trans. Antenna Propagat.*, Vol. 57, No. 9, 2615–2621, Sep. 2009.
23. Wiesbeck, W., M. Younis, and D. Löffler, "Design and measurement of conformal antennas," *IEEE AP-S Int. Symp.*, 84–87, San Antonio, 2002.
24. Raffaelli, S. and M. Johansson, "Conformal array antenna demonstrator for WCDMA applications," *Proceedings of Antenn 03*, 207–212, Kalmar, Sweden, May 2003.
25. Josefsson, L. and P. Persson, *Conformal Array Antenna Theory and Design*, John Wiley & Sons, Inc., New Jersey, 2006.
26. He, Q.-Q. and B.-Z. Wang, "Design of microstrip array antenna by using active element pattern technique combining with Taylor synthesis method," *Progress In Electromagnetics Research*, Vol. 80, 63–76, 2008.